A Mathematical Model for Covalent Proteolysis Targeting Chimeras: Thermodynamics and Kinetics underlying Catalytic Efficiency

Charu Chaudhry[1*]

[1] Molecular & Cellular Pharmacology, Lead Discovery, Janssen Research and Development, LLC , Spring House, PA 19477, United States.

*Corresponding Author

Email: cchaudhr@its.jnj.com; Phone: 1-225-542-3311

Abstract

Proteolysis targeting chimeras (PROTACs), heterobifunctional protein degraders, have emerged as an exciting and transformative technology in chemical biology and drug discovery to degrade disease-causing proteins through co-opting of the ubiquitin-proteosome system (UPS). Here we develop a mechanistic mathematical model for the use of irreversible covalent chemistry in targeted protein degradation (TPD), either to the target protein of interest (POI) or E3 ligase ligand, considering the thermodynamic and kinetic factors governing ternary complex formation, ubiquitination, and degradation through the UPS. We highlight key advantages of covalency to POI and E3 ligase, and the underlying theoretical basis in the TPD reaction framework. We further identify regimes where covalency can serve to overcome weak binary binding affinities and improve kinetics of ternary complex formation and degradation. Our results highlight the enhanced catalytic efficiency of covalent E3 PROTACs and thus their potential to improve the degradation of fast turnover targets.

Introduction

Targeted protein degradation (TPD) has emerged as a powerful therapeutic modality for drug discovery. Small molecule protein degraders hijack the endogenous UPS machinery to promote non-native target recruitment to E3 ubiquitin ligases leading to ligand-dependent target degradation [1-3]. PROTACs consist of a ligand for recruiting a target protein of interest (POI) and an E3 ubiquitin ligase, joined with an appropriate linker. As a result, PROTACs induce proximity between the E3 ligase and POI in a ternary (three -body) complex leading to POI ubiquitination and subsequent degradation by the proteasome [4, 5]. As this mechanism does not rely on functional inhibition, it presents new opportunities to modulate clinically relevant targets that have proven intractable to more traditional methods, such as transcription factors [6-8]. Importantly, TPD has gained significant attention as a revolutionary modality that can outperform traditional small molecule inhibitors and the first degraders are now progressing through human clinical trials [9].

TPD approaches have several potential benefits over direct inhibition of protein targets including improved pharmacodynamics due to the need for resynthesis of the protein target, the abolishment of all functions and interactions of the target due to its degradation, improved selectivity over the target binder alone, and differentiated cellular pharmacology. Importantly, PROTACs have a catalytic mechanism of action, and can be recycled such that one PROTAC molecule can turn over multiple molecules of POI, and thus can exert a substantial pharmacological effect at fractional

2

occupancy of the E3. As a result of this, PROTACs often show higher POI degradation than expected based on their binding affinity to the POI alone. Fractional occupancy also avoids the potential liabilities associated with complete redirection of the E3 ligase from its canonical targets. This catalytic property of degraders has implications that allows for lower therapeutic doses and an improved therapeutic window [6, 10, 11].

Despite these advantages, degrader development and optimization has encountered various challenges, such as weak ligand affinity to the E3 ligase and/or POI, and inefficient catalytic turnover for degradation efficacy. In fact, discovery of potent or covalent small molecules that can be used as E3 ligase recruiting modules have been among some of the largest challenges to expanding TPD scope. In theory, using PROTACs that covalently bind to the POI or E3 could address many of these challenges, which is why covalent PROTACs have begun receiving increasing attention [12]. A number of recent studies have highlighted the discovery of covalent small-molecules that can also be used as E3 ligase recruiting modules to potently degrade target proteins in TPD applications [13-15]. However, to date, there has been no comprehensive theoretical framework to model the effects of covalently targeting the E3 ligase or the POI on PROTAC efficacy, and if one approach yields superior results over the other.

Here, we develop a chemical kinetic model that incorporates covalency into heterobifunctional degraders to gain mechanistic insight into the conditions where irreversible binding warheads to either E3 ligase or POI can offer advantages for TPD (Fig 1). Mathematical treatments of PROTACs have been reported and provide a theoretical framework for degrader (non-covalent) action [16-18]. Herein, we have recapitulated these data and then further extended these models to covalent warheads by allowing irreversible binding/reactivity to occur at any point where E3 ligase or POI is bound to the PROTAC. We hypothesize that a covalent E3 PROTAC, by shifting the equilibrium to the activated E3 ligase complex (E3-PROTAC), stabilizes the repurposed E3 ligase enzyme and primes it to engage and degrade target proteins with increased catalytic efficiency within the thermodynamic cycle of multiple binding steps. We show that covalent E3 PROTACs may also have utility to improve degradation efficiency of fast turnover targets. For ternary complex formation, both covalent E3 and covalent POI binding provide equivalent stabilization. However, for degradation, the covalent E3 PROTAC complex provides a significant advantage under a broad set of conditions, in contrast to the covalent POI based PROTAC which collapses catalytic efficiency to stoichiometric 1:1 PROTAC: POI degradation. Nevertheless, we identify a limited scenario where covalency to the POI can overcome weak binding

3

affinity and confer a benefit in degradation efficacy. We also formulate a notion of catalytic efficiency and show how that can improve in the presence of a covalent E3 PROTAC.

Methods

TPD Mathematical Model overview

Chemical Kinetic Model for Heterobifunctional degrader in TPD

We developed a mechanistic chemical kinetic model in MATLAB based on our current understanding of heterobifunctional protein degrader mechanism-of-action, and a number of simplifying assumptions listed in Figure 2A. A simplified schematic of the model framework is shown in Figure 2B. The core reversible PROTAC model is shown in blue, while irreversibility to E3 ligase is shown in green, and irreversibility to the POI in red. A list of model species is provided in Table 1, and model parameters are summarized in Table 2 along with baseline values and a description of their derivation when applicable. Time dependent ordinary differential equations (ODEs) capturing the various reactions and intermediate species in terms of concentrations, affinities, and rate constants, are detailed in the Supplementary materials.

Binary and ternary complex formation was modeled using mass action kinetics and explicitly defined forward and reverse kinetic rate constants. For the core POI-PROTAC-E3 binding model, we assumed sequential binding steps in which PROTAC associates with either E3 ligase or POI to form a binary complex which can then associate with its other partner to form a ternary complex. All of these binding reactions are reversible. Formation of an irreversibly bound complex followed a two-step process, in which first the PROTAC binds reversibly to its partner, and then a stable covalent bond forms at a given rate. In the irreversible case, a ternary complex can form without regard to whether the covalent bond has formed yet or not; and a covalent bond between PROTAC and its partner can form in either a binary or ternary complex.

In the cellular degradation model, we expand the binding kinetics model with turnover models of POI and E3 ligase, and PROTAC-mediated ubiquitination and degradation steps. Formation of ternary complex leads to POI ubiquitination through a series of steps, which we simplify to a single ubiquitination rate assuming polyubiquitination is processive and fast relative to the first monoubiquitination step. Once the POI is ubiquitinated, the ubiquitinated ternary complex then dissociates at the same rates as non-ubiquitinated ternary, eventually releasing target POI for proteasomal degradation, as well as the E3 ligase and PROTAC for another catalytic cycle in the case of

reversible and covalent E3 PROTAC models. Target protein degradation only occurs following ubiquitination, and ternary complex can dissociate prior to completion of this process, reverting to binary complexes ready to reinitiate the TPD reaction. Notably, we modeled the energetics of ubiquitinated ternary complex formation equivalently to the non-ubiquitinated complex formation, and assumed the proteasome can degrade the ubiquitinated POI, either free or as the binary complex with PROTAC, but not as the ubiquitinated ternary complex due to size constraints. Proteasomal degradation is modeled as a first order exponential decay process. We demonstrate features of the core model by recapitulating various common properties observed experimentally, such as the hook effect and sub-stoichiometric degradation with respect to PROTAC. Our results also align with published modeling studies [7, 10, 16, 19-21]. Sensitivity analyses were also carried out to understand different parameter regimes and their effect on intermediate steps and most importantly degradation efficacy.

The model was implemented in MATLAB R2020a. All simulations were performed using the ODE15s integrator.

Results

Covalent PROTAC stabilizes ternary complex

To begin our investigation, we first considered the ternary complex reaction, and the thermodynamic and kinetic factors that can influence formation of the ternary complex. Building from the analysis of Douglass and coworkers [16], we adapted a four quadrant framework using limiting cases of weak or tight affinity of the PROTAC to either E3 ligase or POI. This naturally leads to four unique combinations of tight binding to both target and ligase, weak to both, and tight to one and weak to other and vice versa. Simulations were performed over a wide range of initial PROTAC concentrations and are shown in Figure 3. Figure 3A shows the fully reversible PROTAC case, modeling ternary complex under equal concentrations of both POI and E3 ligase, and binding affinities set to either 10-fold lower or 10-fold higher than the concentration of each partner's initial condition. Under these conditions, quadrant four (Q4) with tight binding to both arms, showed maximal ternary complex, while Q2 and Q3 showed similar (and much lower) levels of ternary due to symmetry in the initial configuration of the simulations, and Q1 showed minimal ternary complex formation.

We next explored the effect of covalent binding between E3 and PROTAC on ternary complex formation. Figure 3B shows that a covalent E3 PROTAC can provide a significant boost to the

5

stabilization of ternary complex under conditions of low affinity binding to the E3 ligase (Q3). Hence, with a PROTAC that contains a medium-high affinity POI ligand, conversion of a reversible, low affinity E3 ligase ligand to an irreversible covalent binder is predicted to effectively shift the equilibrium towards the ternary complex. However, if a PROTAC also has low affinity to bind the POI, building in covalency toward the E3 ligase does not significantly improve ternary complex formation (compare Q1 and Q2 in Fig 3B vs 3A). Conversely, in the case of PROTACs with weak POI binding (Fig 3C), building covalency to the POI arm may provide significant stabilization of the ternary complex (compare Q2 in 3C vs 3A). It would intuitively follow that converting the lower affinity arm of the PROTAC from a reversible to a covalent ligand would confer the largest benefit in ternary complex and degradation gain.

Covalent E3 PROTAC enhances degradation

We next performed simulations varying E3 ligase affinity over a range of PROTAC concentrations. Evident from the results is that building tighter affinity of the PROTAC for the E3 ligase provided significant improvements in degradation efficacy (Fig 4A) which we are quantifying as the maximum degradation (Dmax=1-Frxn A) at the specified observation time after PROTAC addition. Most irreversible inhibitors bind to their ligand site in two steps, described in classical enzymology by a first reversible step (Ki) before the inactivation step (k_{inact}). Thus, the second order rate constant k_{inact}/ Ki best captures the inhibitory potential for an irreversible inhibitor. To investigate the predictive ability of k_{inact}/Ki in the PROTAC framework, we simulated cases where we varied k_{inact} and Ki respectively. Degradation over a broad PROTAC concentration range was quantified. First, by incorporating an irreversible inactivation step into the E3 ligase PROTAC binding mechanism (k_{inact}=0.1/min), we observed a shift in the steady state to mirror a more potent reversible condition (Fig 4B). In both cases, as the affinity is increased from 10 μM to 1 nM, there is a leftward shift of the peak PROTAC concentration predicted to achieve peak degradation. Notably, at a PROTAC E3 ligase affinity of 1 μM, the addition of an irreversible binding step for the E3 ligase interaction shifted the depth of degradation to exceed that achieved by PROTACs with 0.1 μM E3 ligase binding affinity in the absence of a covalent interaction (compare Fig 4B yellow trace to Fig 4A green trace). Thus, incorporation of a covalent interaction with the E3 ligase can increase the apparent potency of the PROTAC, in this case by over an order of magnitude.

Simulations were also carried out varying the parameters of covalent bond formation rate at a fixed PROTAC E3 ligase affinity (Fig 4C). Notably, increasing k_{inact} or decreasing Ki increases the width of the bell shape degradation curve, with a strong effect of increasing degradation at low concentrations of PROTAC without changing the onset of the hook effect, decreasing degradation at high PROTAC concentrations. We also found that the ratio k_{inact}/Ki is the determining factor for degradation efficacy; i.e. increasing k_{inact} or decreasing Ki while maintaining the same k_{inact}/Ki ratio, does not lead to a change in degradation potency (Fig 4D). Furthermore, increasing k_{inact}/Ki can significantly improve degradation. In Figure 4E for example, increasing k_{inact}/Ki by an order of magnitude led to a significant increase in Dmax by ~ 60% at 6 hr (compare Fig 4D to 4E). These studies so far are focused on the fast ternary kinetics regime with diffusion limited on-off rates. Future investigation into other kinetic regimes is also warranted where we anticipate Ki or k_{inact} may drive improvements in degradation.

Covalent E3 PROTAC that co-opts an E3 ligase with a long half-life provides greater degradation efficacy

One of the target selection considerations for a TPD approach is a long POI half-life, which enables efficient protein knockdown and a durable pharmacodynamic benefit [2, 3, 11]. Extending this to utilization of covalent E3 ligase PROTACs and E3 ligase selection, the intrinsic turnover of the E3 ligase is also predicted to play a role in degradation efficacy. This is demonstrated in Figure 5 whereas E3 half-life is increased, deeper degradation over a broader PROTAC concentration range is achieved. Therefore, greater degradation efficacy is achieved with a longer half-life E3 ligase that has been modified by a covalent PROTAC. Notably, a shorter E3 ligase half-life is expected to result in faster loss of the covalent PROTAC degrader from the system. Conversely, a PROTAC with poor pharmacokinetics (PK), by covalently engaging the E3, could benefit from enhanced PK properties.

Carrying out these simulations at various E3 ligase half-life values, maximum degradation achieved plotted as a function of E3 ligase half-life (Fig 5C) also revealed that there is a finite benefit to a longer E3 ligase half-life, beyond which there is no further benefit. This set point is determined by various parameters both downstream and upstream of the covalent binding step, such as ubiquitination rate as well as POI resynthesis rate. Notably, a non-zero plateau is observed because of target resynthesis. This kind of analysis can help in selection of E3s for a covalent PROTAC approach [22, 23].

PROTAC covalent to the target stabilizes ternary complex but has limited advantage for target degradation

From the simulations in Figure 3, we observed that a PROTAC with a weak POI binder, when converted into a covalent POI binder, confers ternary complex stabilization. We then considered how stabilized covalent POI ternary complex translates into degradation efficacy, given stoichiometric target degradation.

To address this, we modified the TPD mathematical model to allow irreversible binding to occur at any point where POI is bound to the PROTAC in a manner analogous to how we previously modeled covalent E3 ligase binding (Fig 2, covalent target model in red). Notably, an important difference between the two models is that, in contrast to a covalent E3 ligase PROTAC, a PROTAC incorporating covalent POI binding is not recycled back for multiple POI degradation cycles. We carried out four quadrant simulations under both low and high affinity conditions to the POI and the E3 ligase. In Figure 6A, as seen previously, covalent binding to the E3 ligase significantly boosted degradation efficacy in the context of a weak E3 binder (see Q1 and Q3). Notably, under already tight binding to the E3 ligase, covalency to the E3 did not comparatively offer benefit (Q2 and Q4). Still, for the covalent E3 PROTAC, covalent conditions are never worse than the non-covalent scenario. In contrast to this, when we simulate covalent POI binding (Fig 6B), only in the limiting case of weak POI binding did covalency yield an improvement in degradation over the non-covalent scenario. In the majority of conditions tested, building in covalency to the POI into the model is in fact worse than the corresponding noncovalent POI PROTAC. Notably, when there is already tight binding to the POI, there is a penalty for irreversible POI binding due to consumption of the PROTAC on every cycle of target degradation.

Importantly, as discussed above, at the ternary level, equivalent stabilization of the ternary complex is observed whether the covalent partner is targeted to either the E3 ligase or the POI (Fig 3 B, C). However, the ubiquitination and degradation steps introduce asymmetry in the catalytic cycle and the desired properties for PROTAC binding to the POI and E3 ligase diverge. This is underscored by the observed enhancement in degradation in the covalent E3 ligase case versus the thermodynamically analogous covalent POI case (Fig 6A Q3 vs 6B Q2). We hypothesize this originates in large part due to differences in PROTAC consumption between the two scenarios. In addition, we suggest that increased catalytic efficiency intrinsic to the activated E3 ligase complex (E3-covalent PROTAC) may also play a contributing role. We will explore these hypotheses using kinetic simulations later in this study.

Enhanced degradation efficacy of covalent E3 PROTAC offers advantage to degrade faster turnover protein targets

We have established that a covalent E3 PROTAC can confer significant advantages to degradation efficacy for a target protein. Since all of our simulations so far have been carried out using target proteins with a relatively long half-life value of 24 hr, we tested how generalizable this advantage can be for targets with shorter half-lives, (*i.e.* faster turnover proteins). Figure 7 shows simulated degradation results for a target with a half-life of 1 hour, considering both reversible and covalent E3 ligase PROTAC mechanisms using the four-quadrant framework of weak and tight affinity to POI and E3 ligase. In the reversible case, it is difficult to achieve any significant depth of degradation except for the tight E3 ligase-tight target binding conditions, but the results are still not equivalent to the degradation achieved for a 24-hour half-life POI (see pink trace in Fig 6A, Q4). Notably, when covalency is incorporated into the E3 ligase ligand, significant degradation is restored (Dmax= ~80% for Target $T_{1/2}$=1 hour vs 100% for Target T1/2=24 hour). Not surprisingly, lower POI levels were achieved across a broader PROTAC concentration range for target with $T_{1/2}$ 24 hours vs 1 hour. Nonetheless, a covalent E3 ligase PROTAC enables efficient target protein degradation even for fast turnover targets, whereas a reversible PROTAC cannot achieve the necessary catalytic efficiency to effectively compete with fast target protein resynthesis rates. Thus, a covalent E3 PROTAC strategy may be an attractive option to pursue for fast turnover targets. Of course, as demonstrated in earlier simulations (Fig 5), E3 ligase turnover itself should also be taken into account in E3 ligase selection for such an approach.

Reaction kinetics: covalent bond formation, degradation and PROTAC consumption

To understand the interplay between the kinetics of covalent bond formation to E3 ligase/POI and degradation, we next compared the dynamics of each species in the system (Fig 8). We leveraged these simulations to gain insight into the formation and dissipation of key ternary and ubiquitinated species in the reaction, which are more challenging to measure experimentally. Notably, both covalent POI and E3 cases exhibit an initial transient increase in total ternary and ubiquitinated species with similar temporal profiles and greater magnitude in the covalent E3 case (Fig 8 B,C), while for the reversible case the transient for both species is flat (Fig 8A). In the case of a covalent E3 ligase PROTAC, total ternary and ubiquitinated species both reach a similar steady state and >99% POI degradation is achieved in 3 hours (Fig 8B). In contrast in the covalent POI PROTAC scenario, the disappearance of

9

PROTAC occurs significantly more rapidly, leading to a concomitant rapid loss of ternary and ubiquitinated species that coincides with recovery in target levels (Fig 8C). This is because PROTAC is consumed in every cycle of target degradation, driving down the available PROTAC concentration remaining in the system. Over the course of the reaction, >99% of covalent POI PROTAC is consumed, in contrast to only ~ 30% of total PROTAC loss due to turnover of the covalent E3 ligase-PROTAC complex under similar conditions.

To test the difference in degradation efficacy between a covalent E3 ligase-PROTAC and a "regenerating" covalent POI-PROTAC, we tested the hypothetical case where a fully functional PROTAC can be regenerated during proteasomal degradation of the POI instead of being irreversibly lost on turnover of the covalent POI-PROTAC complex. This approximates the case of a reversible covalent inhibitor. As shown in the simulation results in Fig 8D, total PROTAC is now no longer consumed during the reaction. Greater depth of degradation is observed for the covalent POI- PROTAC regeneration case versus the original covalent POI PROTAC (compare 8D vs 8C), but this still falls short of the covalent E3 ligase PROTAC (Fig 8B) by ~2 fold. We hypothesize that the ~ two-fold enhancement in degradation in the covalent E3 ligase system is due to greater catalytic cycling, underscoring the true catalytic benefit from stabilizing the activated ligase complex. This value will likely be dependent on specific system parameters.

Discussion

There has been increasing interest in covalent PROTACs, however the developability of selective potent covalent degraders remains challenging [24, 25]. The reductionist mechanistic model we present here provides a framework to understand heterobifunctional degrader mechanism of action for covalent TPD degraders, utilizing covalent moieties towards either POI or E3 ligase. Specific advantages of covalent PROTACs emerged through these simulations, providing both theoretical corroboration of experimental findings that have been previously reported in the literature as well as new insights. Our results demonstrate that a covalent E3 ligase PROTAC can overcome weak E3 ligase binding affinity and stabilize ternary complex, resulting in an increase in degradation efficacy. Despite equivalent ternary complex stabilization, covalency to the E3 ligase can enhance catalytic cycling of the E3 while covalency to the POI ablates the catalytic benefit. Nonetheless, a covalent POI PROTAC still has some limited advantages to overcome weak target binding resulting in a boost in ternary complex concentration that

10

can promote degradation. We also simulated key mechanistic intermediates in the reaction cycle, providing insights into the link between the kinetics of covalent bond formation, ternary complex, ubiquitination, and degradation. These kinetic simulations demonstrated that covalent binding to trap the E3 ligase-PROTAC binary complex can improve the kinetics of ternary complex formation and ubiquitination, and as a result degradation kinetics. This can be understood considering that an irreversible E3 PROTAC complex can recruit multiple POI molecules for ubiquitination and degradation, without the need for the prior kinetic step of forming the E3 PROTAC interaction. Furthermore, our results demonstrate that target degradation depends upon the intrinsic values of E3 ligase and target turnover. For slow turnover targets, this effectively decouples the pharmacokinetics from the pharmacodynamics.

It has been suggested that fractional target engagement can provide maximal degradation, but this has not been carefully examined. We can use the model described here to quantitatively evaluate the relationship of E3 occupancy and degradation. In Figure 9, we calculate target degradation and correlate with fractional occupancy of the E3 ligase as a function of time. The results clearly demonstrate that high levels of target degradation can be achieved while engaging fractional E3 ligase. For example, in Fig 9C, > 90% target loss can be achieved with as little as 30% of the available E3 ligase, preserving 70% of the ligase in a non-modified form to carry out its normal functions. Notably, the separation in the time-courses between target degradation and E3 occupancy increase with decreasing inactivation rate (k_{inact}), for the same Ki. We also observe an increase in time to maximum degradation as k_{inact} decreases. We can define a catalytic efficiency (CE) as target protein degraded per E3 occupied with PROTAC (PE+PE*). Note the catalytic efficiency itself is time dependent. Maximum target degradation is achieved with the fastest k_{inact} rate, however this has the lowest CE because 70% of the E3 ligase is bound with PROTAC (Fig 9A). In contrast, the slowest k_{inact}, leads to 12% E3 occupancy and 68% target degradation (Fig 9D), producing the highest catalytic efficiency but at the expense of total degradation. We also note that time to maximal degradation is 24 hours in the latter case versus only 4 hours in the former fastest k_{inact} case (Fig 9D vs A). This highlights the need to study these systems from many perspectives; i.e. just having the most efficient degrader may not be the optimal degrader.

Several proof-of-concept studies reporting covalent ligands for the recruitment of E3 ligases and targets have been carried out. These experimental data offer the opportunity to qualitatively validate our model, however, to date published kinetic data is unavailable that would enable more quantitative comparisons. For PROTACs with covalency to the POI, Zeng et al. for example developed KRASG12C

degraders based on the covalent inhibitor ARS1620, since potent noncovalent binders were not available owing to the lack of well-defined pockets on KRAS [26]. This finding represents the case of Q2 in Fig6B, demonstrating as the model predicts that low binding affinity of a noncovalent ligand can be enhanced with covalency. For PROTACs with covalency to the E3, an electrophilic PROTAC KBO2-SLF was identified to covalently engage DCAF16 E3 with low fractional occupancy and yet robustly degrade BRD4 [15], consistent with the predictions of our model (Fig 9). Another similar example has been reported for nimbolide [27], a terpene natural product based covalent recruiter of RNF114 E3 ligase, that when incorporated into a BCR ABL directed PROTAC, demonstrates robust degradation efficacy. This finding represents the case of Q3 in Fig 6A, where a covalent E3 binder enhances degradation in context of a high affinity POI binder.

The examples above demonstrate that partial occupancy can lead to efficient degradation in vitro. One of the challenges with a covalent E3 mechanism however is the potential to drive full occupancy of the E3 which could result in increased mechanism-based toxicity. Thus, an important consideration is maintaining an appropriate PROTAC dose that leads to degradation efficacy without fully saturating all of the E3. A covalent E3 PROTAC is the limiting case of an E3 binder with an infinitesimal off-rate. An attractive strategy that combines the benefit of a covalent E3 ligand with the super-stoichiometric target degradation, could be conversion to a covalent reversible E3 ligand that offers potential for sustained target engagement, while mitigating toxicity effects caused by permanent protein modification. In fact, the first covalent reversible E3 ligase recruiter, a bifunctional small molecule linking KEAP-NRF2 activator bardoxolone to BRD4 inhibitor JQ1 [28], has been reported. Another attractive feature of a covalent E3 PROTAC mechanism is the potential to effectively convert from a three body to a pseudo two body system, by modulating k_{inact} rate relative to degradation (k_{deg}) rate. This could allow for a low enough efficacious dose to negate the hook effect normally associated with bifunctional degraders. While we have explored k_{inact}/Ki as the primary factor driving degradation efficacy under fast ternary kinetics, there may be regimens of binding, dissociation, and proteolytic processing in which k_{inact} is the primary determinant of degradation efficacy. Additional work will take into consideration a full analysis of kinact, Ki and degradation rates in different kinetic regimes.

In summary, we have developed a mechanistic model for reversible and irreversible PROTACs, incorporating thermodynamic and kinetic factors that govern heterobifunctional degrader efficacy and catalytic efficiency. This provides a framework to understand PROTAC mechanism of action and gain both intuitive and non-intuitive insights into optimal degrader properties, while also presenting an

exciting opportunity to tune PROTAC design to the requirements of the target system. Notably, while molecular glues are outside the scope of our current study, we would expect similar principles of covalent modification of the E3 to translate there. Through modeling, we can examine any E3 and target system and probe various steps in the TPD reaction, including the kinetics of PROTAC binding and covalent bond formation to the E3/target, ternary complex formation and ubiquitination, leading to degradation. Requirements of k_{inact}/Ki for a particular system will depend on target and E3 half-lives, compound PK, stoichiometry between E3 and target, and the degradation threshold for efficacy. The model has the potential to explore many parameters and generate testable predictions that can drive experimental design of covalent PROTACs. Collectively, our analyses suggest specific advantages of covalent PROTACs, the proof of which we expect to translate to improvement of degradation efficacy in vivo and ultimately the clinic.

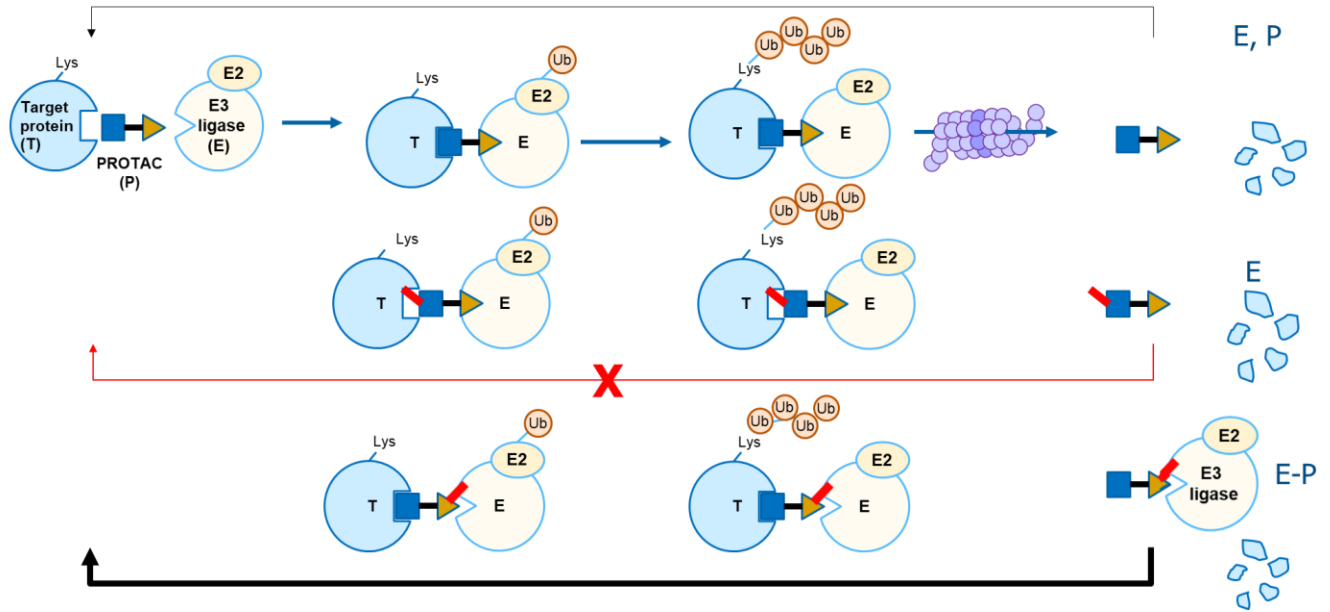**Acknowledgements**

Figures

Figure 1

Fig 1. Schematic mechanisms for PROTAC induced targeted protein degradation (TPD) utilizing reversible chemistry or irreversible covalent engagement to E3 ligase or target protein. Covalent binding (red connection) to the target leads to stoichiometric degradation because the PROTAC is lost with each round of degradation. PROTACs that are fully reversible or those that engage the E3 ligase via an irreversible covalent bond can lead to sub-stoichiometric degradation. This is because each PROTAC molecule can be used to degrade many molecules of target. The electrophile is indicated with red linker, the target binder is colored in blue, and E3 ligase binder in brown.

Figure 2

A

> *Assumptions:*
>
> 1. Reduce complexity of E1-E2-E3 ubiquitination cascade into single effective ubiquitination rate (k_{ub}), focused on E2-E3 ubiquitination of substrate
>   - Polyubiquitination is processive and fast relative to 1st monoubiquitination
>   - Once POI is ubiquitinated, $T_{ub}PE$ energetics is the same as TPE
> 2. All ubiquitination is productive and leads to degradation
> 3. Proteosome recognizes T_{ub} and $T_{ub}P$, but not $T_{ub}PE$.
> 4. Proteosome degradation modeled by simple 1st order exponential decay

B

T=target
P=PROTAC
E=E3 Ligase
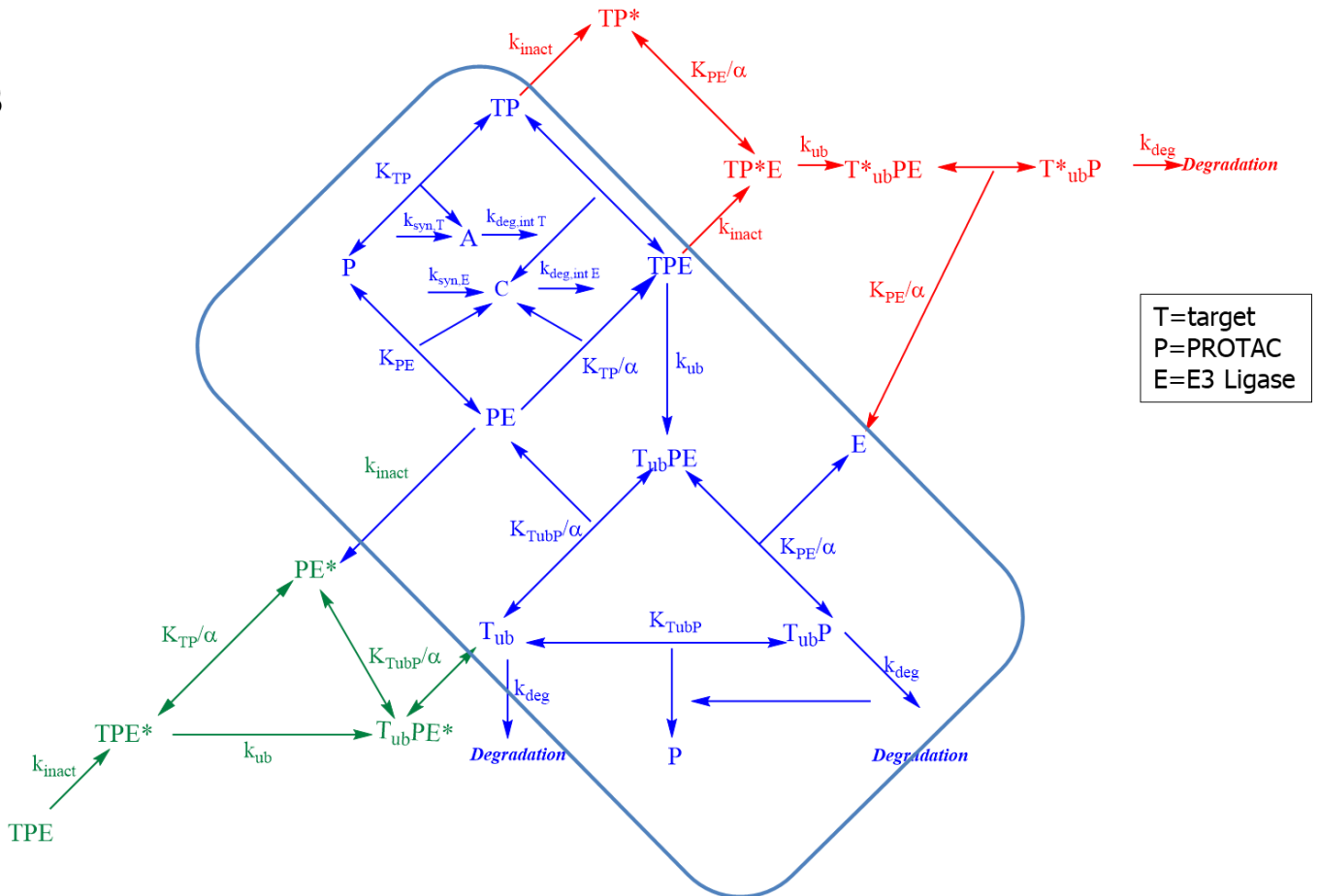
Fig 2. Chemical Kinetic Model for PROTAC induced TPD for both reversible and irreversible chemistries. (a) Assumptions of the model. (b) Core Reversible model is shown in blue, Covalent E3 Ligase model in green, and Covalent Target model in red. T represents target protein, P represents

PROTAC, and E represents E3 ligase. Double-headed arrows represent reversible reactions whereas irreversible reactions are represented by single arrows. Species and parameters are listed in Table 1 and 2 respectively.
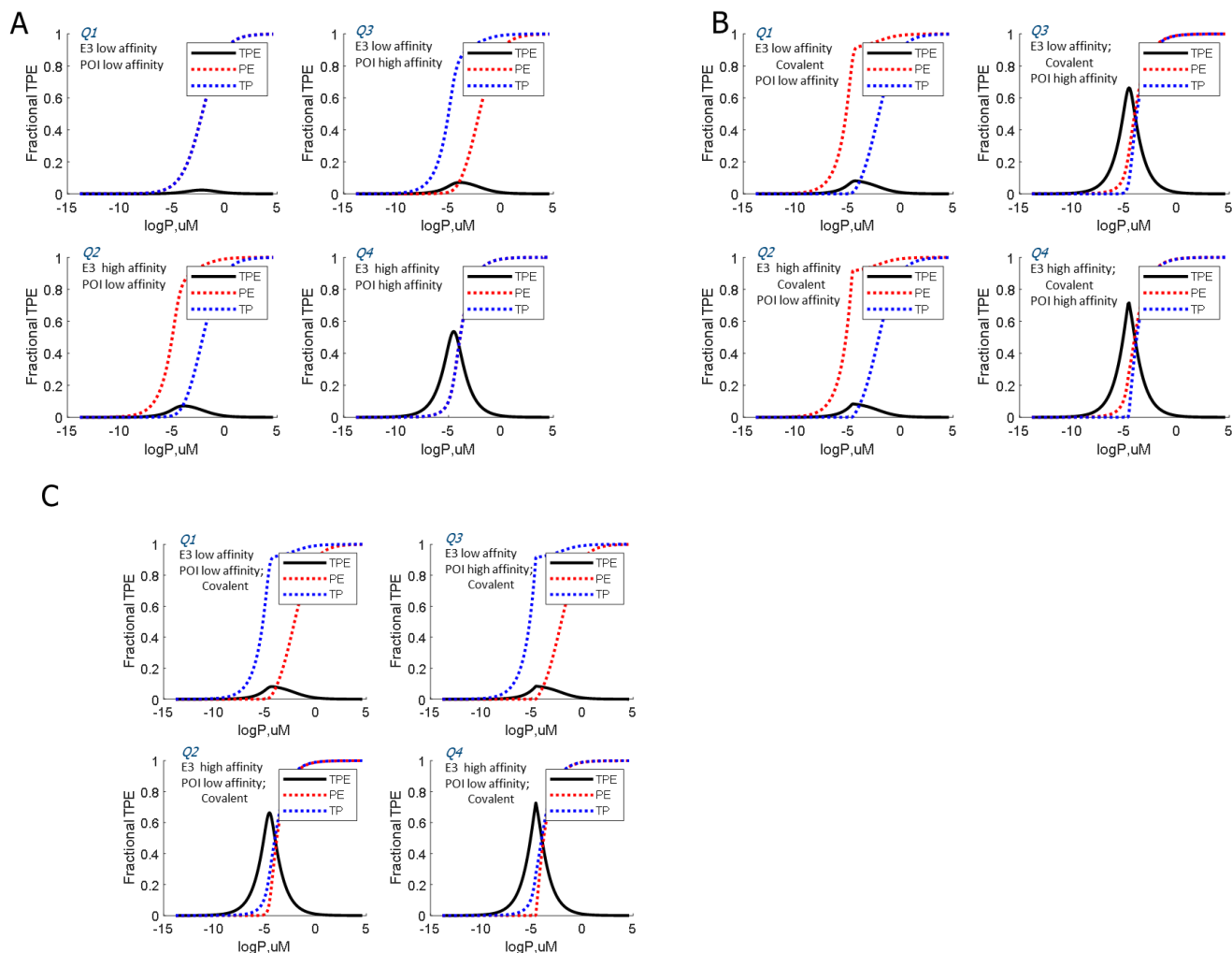
Figure 3

Fig 3. **Simulations of ternary complex formation.** Plots showing the fraction ternary complex (TPE) as a function of PROTAC concentration using: (A) reversible binding, (B) covalent-E3 binding, and (C) covalent-target binding. Binary target-PROTAC (TP) and PROTAC-E3 (PE) complexes are also shown as dotted curves. Simulation parameters are [T]=[E]=0.01 μM, k_{on}=6000 μM^{-1}min^{-1}, with binary affinities (K_{TP} and K_{PE}) as follows based on quadrant: Q1 K_{TP}=K_{PE}=1 μM; Q2 K_{TP}=1 μM, K_{PE} =0.01 μM; Q3 K_{TP} =0.01 μM, K_{PE} =1 μM; Q4 K_{TP} =0.01 μM, K_{PE} =0.01 μM. For covalent reactions, k_{inact}=0.1 min^{-1}.
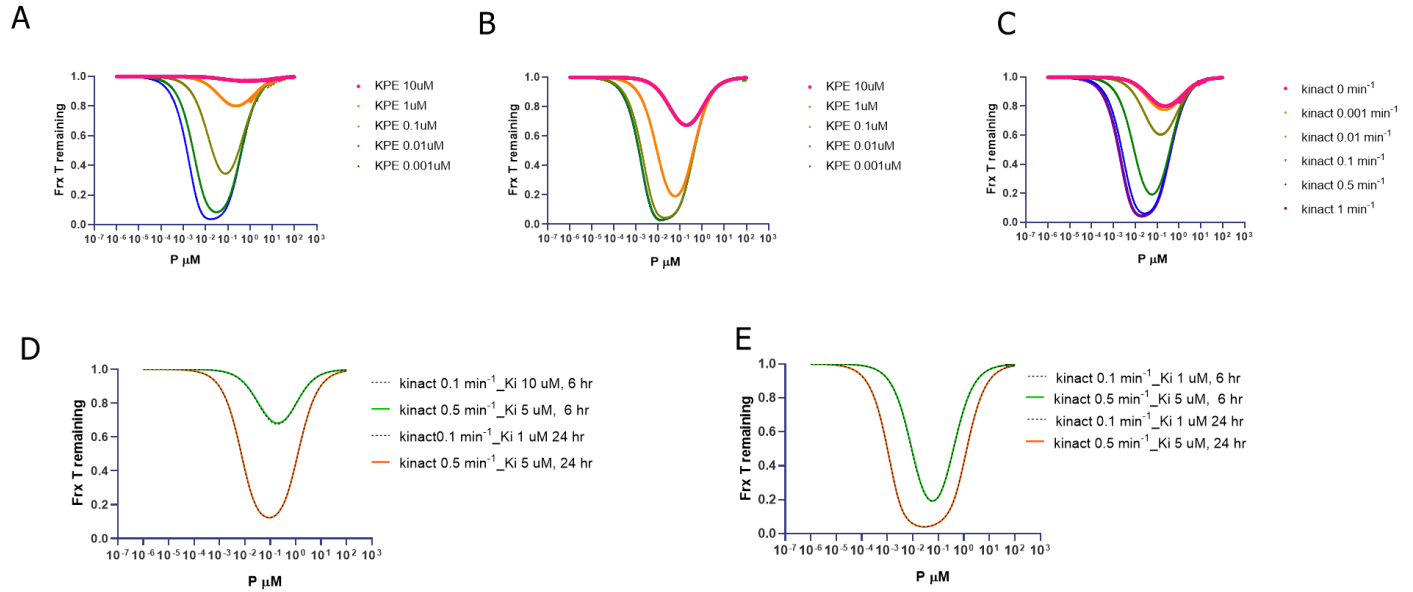
Figure 4

Fig 4. **Covalent E3 PROTAC significantly enhances degradation.** (A,B) The fraction of target remaining at 6hr varying PROTAC-E3 binding affinity (A) without, or (B) with covalent bond formation (k_{inact}=0.1 min^{-1}). (C) The fraction of target remaining after 6hr varying the K_{inact} rate of covalent PROTAC-E3 compounds (fixed E3 affinity K_{PE}= 1uM). (D) The fraction of target remaining as a function of k_{inact}/Ki of 0.01 μM^{-1} min^{-1}, and (E) k_{inact}/Ki of 0.1 μM^{-1} min^{-1} at 6 and 24 hr. K_{TP}=0.05 μM, while K_{PE} varied from 10 to 0.001 μM; other simulation parameters include k_{on} for binary complex (TP, PE) =6000 min$^{-1}\mu M^{-1}$; k_{inact}=0.1 min^{-1}, k_{ub}=0.1 min^{-1}, kdeg= 1 min^{-1}
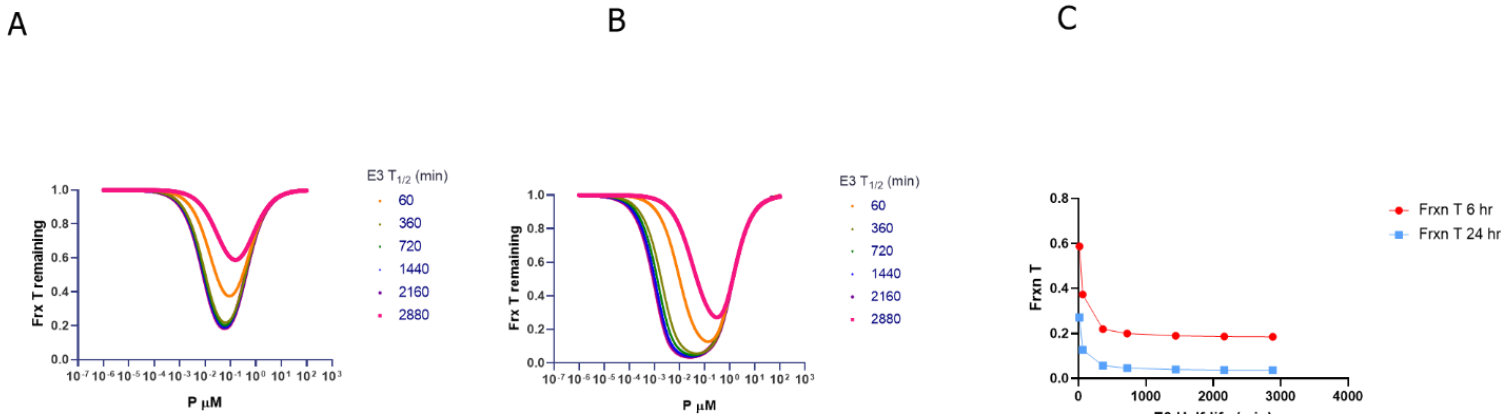
Figure 5

Fig 5. **Effect of E3 ligase half-life on degradation efficacy. (A,B)** The fraction of target degraded is plotted after (A) 6hr, and (B) 24hr at various E3 half-lives ranging from 1, 6, 12, 24, 36, 48 hr. Simulation

parameters are [T]=[E]=0.01 μM, target half-life=24 hr, binary affinities of K_{TP}=0.05 μM and K_{PE}= 1 μM; k_{on} for binary complex (TP, PE) =6000 min^{-1}μM^{-1}; k_{inact}=0.1 min^{-1}, k_{ub}=0.1 min^{-1}, k_{deg}= 1 min^{-1}. **(C)** Plot of maximum degradation at 6 and 24 hr across different E3 half-lives.
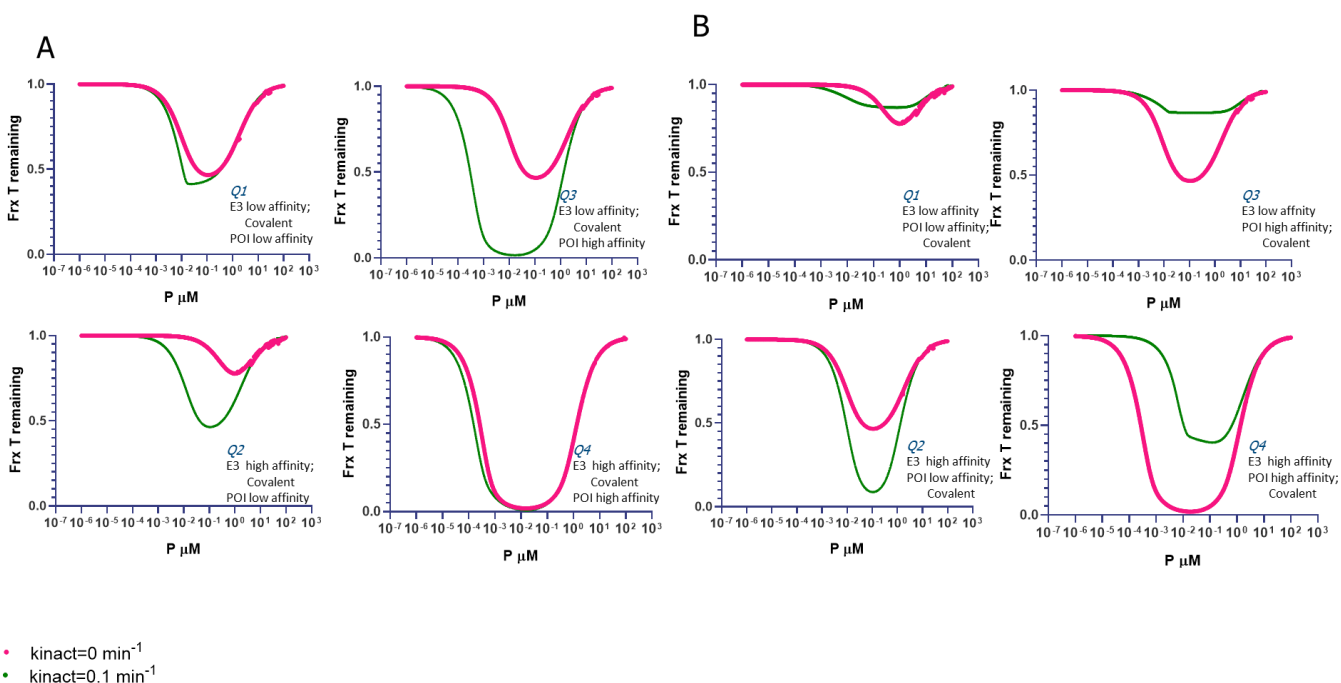
Figure 6

Fig 6. Comparison of PROTAC degradation efficacy for Covalent E3 (A) vs Covalent POI binder (B) systems. The four quadrant framework is utilized, with affinities as follows: Q1 K_{TP}=K_{PE}=1 μM, Q2 K_{TP} =1 μM, K_{PE} =0.01 μM, Q3 K_{TP}=0.01 μM, K_{PE} =1 μM, and Q4 K_{TP}= K_{PE} =0.01 μM, for target and E3 with half-lives of 24 hr. Both reversible (pink) and covalent E3 (k_{inact}=0.1 min^{-1}; green) conditions are shown for each binding affinity pair. Global simulation parameters include [T]=[E]=0.01 μM, k_{on}=6000 μM^{-1}min^{-1}, k_{ub}=0.1 min^{-1}, k_{inact}=0.1 min^{-1}, k_{deg}=1 min^{-1}
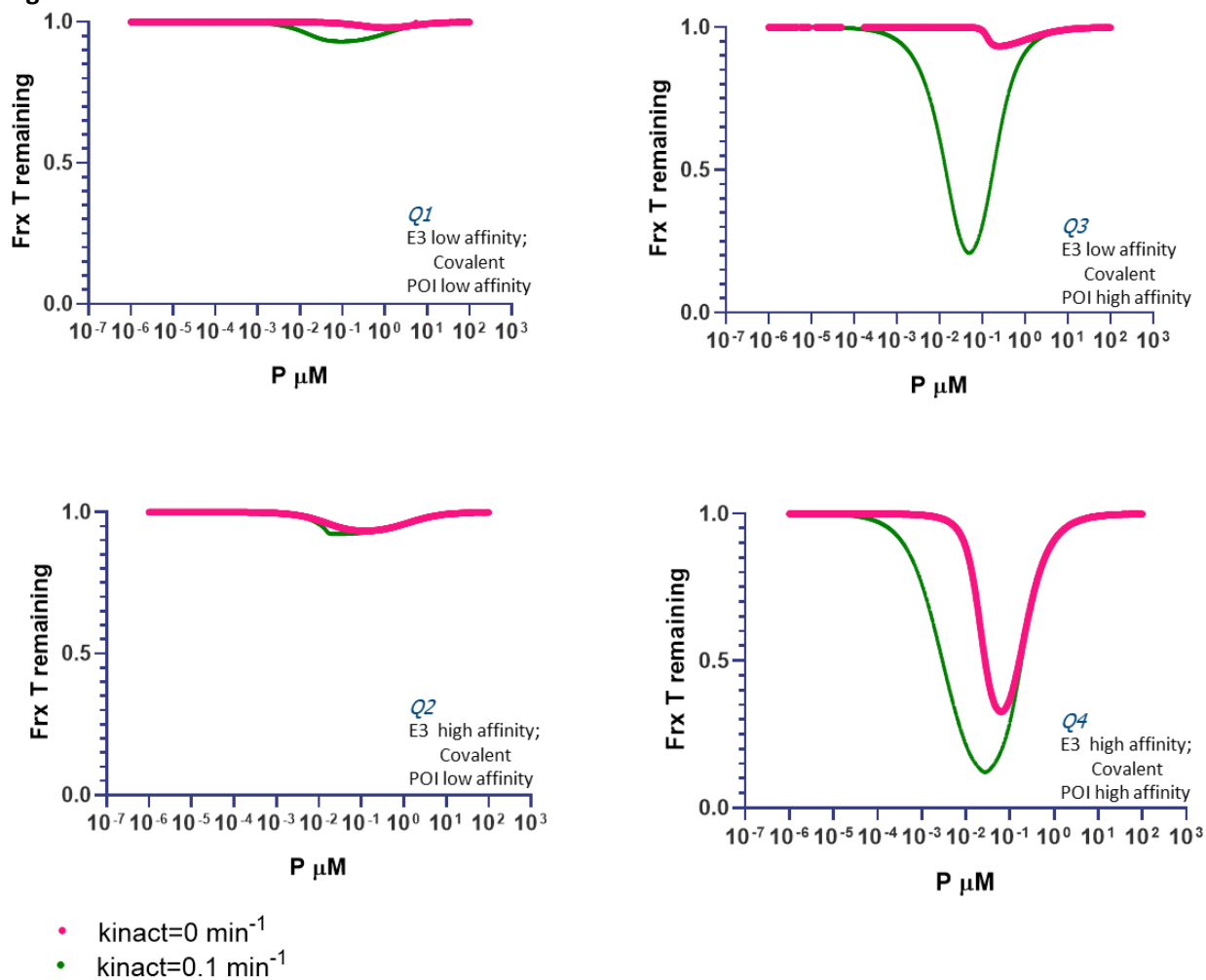
Figure 7

Fig 7. Covalent E3 PROTAC can compete with fast resynthesis rate of short half-life target.

Fraction of target degraded by covalent E3 PROTAC is plotted at 24 hr, for a target with a short half-life of 60 min. The four quadrants represent different affinities as follows: Q1 $K_{TP}=K_{PE}=1$ μM, Q2 $K_{TP}=1$ μM, $K_{PE}=0.01$ μM, Q3 $K_{TP}=0.01$ μM, $K_{PE}=1$ μM, and Q4 $K_{TP}=K_{PE}=0.01$ μM. Both reversible (pink) and covalent E3 ($k_{inact}=0.1$ min^{-1}; green) conditions are shown for each binding affinity pair.
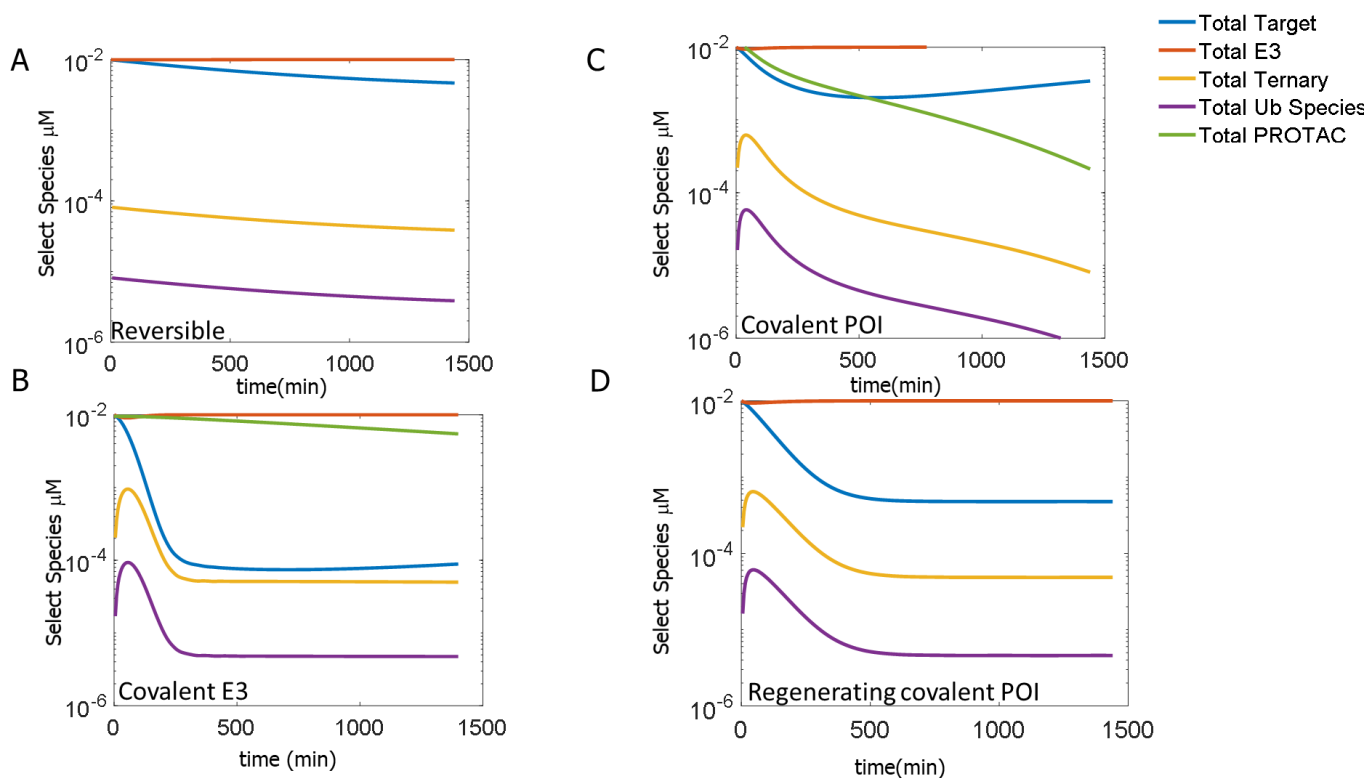
Figure 8

Fig 8. Kinetic simulations of Reversible and Covalent E3 and POI TPD reactions. Timecourses **following total target, E3 ligase, and key ternary and ubiquitinated species intermediates** are shown under the following conditions: fully reversible (no inactivation); K_{TP}= 0.01 μM K_{PE}= 1uM (A) ; covalent E3 binding; K_{PE} = 1 μM, K_{TP} = 0.01μM (B) ; covalent target binding; K_{PE} =0.01 μM, K_{TP} = 1 μM (C), same as C but allow regeneration of the PROTAC after a single round of target degradation (D). Global simulation parameters include [T]=[E]=0.01 μM, target half-life=24 hr, E3 half-life=24 hr, k_{on}=6000 μM^{-1}min^{-1}, k_{ub}=0.1 min^{-1}, k_{inact}=1 min^{-1} , k_{deg}=1 min^{-1}, with binary affinities varying as described above.

Figure 9

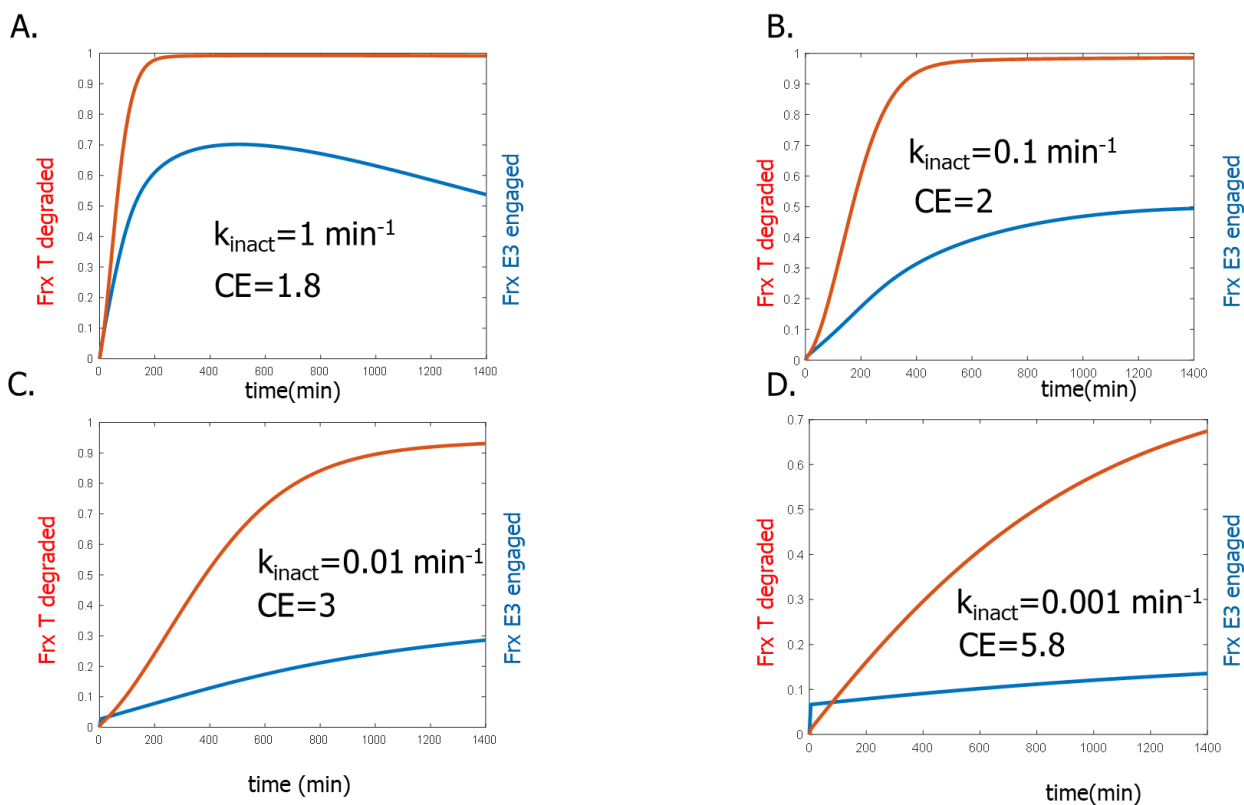**Fig.9. Target Degradation and Fractional E3 Occupancy. Kinetic simulations are carried out at fixed Ki** (K_{TP} =0.01 µM and K_{PE} =1 µM) and varying covalent E3 inactivation rate. Traces are shown at a single concentration of PROTAC that corresponds to peak ternary. Different covalent inactivation rate of E3 (kinact_PE) tested are : 1 min^{-1} (A), 0.1 min^{-1} (B), 0.01 min^{-1} (C), 0.001 min^{-1} (D). Catalytic efficiency (CE) is calculated as target protein degraded per E3 bound to PROTAC (PE+PE*). Simulation parameters include [T]=[E]=0.01 µM, target half-life=24 hr, E3 half-life=24 hr, k_{on}=6000 uM^{-1} min^{-1}, k_{ub}=0.1 min^{-1}, k_{deg}=1 min^{-1}.

Table 1 : List of Model Species

Species	Description	Units	Model
T	Target	μM	Core
P	PROTAC	μM	Core
E	E3 Ligase	μM	Core
TP	Target-PROTAC binary complex	μM	Core
PE	E Ligase-PROTAC binary complex	μM	Core
TPE	Ternary Complex of Target-PROTAC-E3 Ligase	μM	Core
TubP	Ubiquitinated Target-PROTAC	μM	Core
TubPE	Ternary Complex with Ubiquitinated Target	μM	Core
Tub	Ubiquitinated Target	μM	Core
Tdeg	Amount of target degraded	μM	Core
T*P	Covalent Target-PROTAC binary complex	μM	Covalent Target
T*PE	Ternary complex with covalent bond between Target and PROTAC	μM	Covalent Target
T*ubPE	Ternary complex with covalent bond between ubiquitinated Target and PROTAC	μM	Covalent Target
T*ubP	Binary complex of ubiquitinated target covalently bound to PROTAC	μM	Covalent Target
PE*	Covalent E3 Ligase-PROTAC binary complex	μM	Covalent Ligase
TPE*	Ternary complex with covalent bond between E3 ligase and PROTAC	μM	Covalent Ligase
TubPE*	Ternary complex with ubiquitinated target and covalently bound E3 Ligase-PROTAC	μM	Covalent Ligase

Table 2: Model Parameters

Name	Description	Value or range	Units	Comment
T0	Initial concentration of target	0.01	μM	
E0	Initial concentration of E3 ligase	0.01	μM	
K_{TP}	Binding affinity of target-PROTAC complex	0.001-10	μM	
K_{PE}	Binding affinity of E3 ligase-PROTAC complex	0.001-10	μM	
kon	association rate	6000	$\mu M^{-1}.min^{-1}$	
kinact	Inactivation rate	0-1	min^{-1}	
alpha	Cooperativity factor	1-10	unitless	
koff_T_P	dissociation rate of AB-> A+B		min^{-1}	kon*Kab
koff_P_E	dissociation rate of BC-> B+C		min^{-1}	kon*Kbc
koff_T_PE	dissociation rate of ABC-> A+BC		min^{-1}	kon*Kab/alpha
koff_TP_E	dissociation rate of ABC-> AB+C		min^{-1}	kon*Kbc/alpha
kub	Ubiquitination rate		min^{-1}	
kdeg	Degradation rate	0.1-1	min^{-1}	
$kdeg_{int}$	Intrinsic degradation rate		min-1	Calculated from half-life

References

1. Churcher, I., *Protac-Induced Protein Degradation in Drug Discovery: Breaking the Rules or Just Making New Ones?* J Med Chem, 2018. **61**(2): p. 444-452.
2. Chamberlain, P.P. and L.G. Hamann, *Development of targeted protein degradation therapeutics.* Nat Chem Biol, 2019. **15**(10): p. 937-944.
3. Pettersson, M. and C.M. Crews, *PROteolysis TArgeting Chimeras (PROTACs) - Past, present and future.* Drug Discov Today Technol, 2019. **31**: p. 15-27.
4. Edmondson, S.D., B. Yang, and C. Fallan, *Proteolysis targeting chimeras (PROTACs) in 'beyond rule-of-five' chemical space: Recent progress and future challenges.* Bioorg Med Chem Lett, 2019. **29**(13): p. 1555-1564.
5. Paiva, S.L. and C.M. Crews, *Targeted protein degradation: elements of PROTAC design.* Curr Opin Chem Biol, 2019. **50**: p. 111-119.
6. Bondeson, D.P., et al., *Catalytic in vivo protein knockdown by small-molecule PROTACs.* Nat Chem Biol, 2015. **11**(8): p. 611-7.
7. Hughes, S.J. and A. Ciulli, *Molecular recognition of ternary complexes: a new dimension in the structure-guided design of chemical degraders.* Essays Biochem, 2017. **61**(5): p. 505-516.
8. Bondeson, D.P., et al., *Lessons in PROTAC Design from Selective Degradation with a Promiscuous Warhead.* Cell Chem Biol, 2018. **25**(1): p. 78-87 e5.
9. Mullard, A., *Targeted protein degraders crowd into the clinic.* Nature Reviews Drug Disocvery, 2021. **20**(April): p. 247-250.
10. Fisher, S.L. and A.J. Phillips, *Targeted protein degradation and the enzymology of degraders.* Curr Opin Chem Biol, 2018. **44**: p. 47-55.
11. Mares, A., et al., *Extended pharmacodynamic responses observed upon PROTAC-mediated degradation of RIPK2.* Commun Biol, 2020. **3**(1): p. 140.
12. Grimster, N.P., *Covalent PROTACs: the best of both worlds?* RSC Medicinal Chemistry, 2021.
13. Spradlin, J.N., et al., *Harnessing the anti-cancer natural product nimbolide for targeted protein degradation.* Nat Chem Biol, 2019. **15**(7): p. 747-755.
14. Ward, C.C., et al., *Covalent Ligand Screening Uncovers a RNF4 E3 Ligase Recruiter for Targeted Protein Degradation Applications.* ACS Chem Biol, 2019. **14**(11): p. 2430-2440.
15. Zhang, X., et al., *Electrophilic PROTACs that degrade nuclear proteins by engaging DCAF16.* Nat Chem Biol, 2019. **15**(7): p. 737-746.
16. Douglass, E.F., Jr., et al., *A comprehensive mathematical model for three-body binding equilibria.* J Am Chem Soc, 2013. **135**(16): p. 6092-9.
17. Bartlett, D.W. and A.M. Gilbert, *A kinetic proofreading model for bispecific protein degraders.* J Pharmacokinet Pharmacodyn, 2020.
18. Han, B., *A suite of mathematical solutions to describe ternary complex formation and their application to targeted protein degradation by heterobifunctional ligands.* J Biol Chem, 2020. **295**(45): p. 15280-15291.
19. Riching, K.M., et al., *Quantitative Live-Cell Kinetic Degradation and Mechanistic Profiling of PROTAC Mode of Action.* ACS Chem Biol, 2018. **13**(9): p. 2758-2770.
20. Zorba, A., et al., *Delineating the role of cooperativity in the design of potent PROTACs for BTK.* Proc Natl Acad Sci U S A, 2018. **115**(31): p. E7285-E7292.
21. Roy, M.J., et al., *SPR-Measured Dissociation Kinetics of PROTAC Ternary Complexes Influence Target Degradation Rate.* ACS Chem Biol, 2019. **14**(3): p. 361-368.

22. Gabizon, R. and N. London, *The rise of covalent proteolysis targeting chimeras.* Curr Opin Chem Biol, 2021. **62**: p. 24-33.
23. Belcher, B.P., C.C. Ward, and D.K. Nomura, *Ligandability of E3 Ligases for Targeted Protein Degradation Applications.* Biochemistry, 2021.
24. Tinworth, C.P., et al., *PROTAC-Mediated Degradation of Bruton's Tyrosine Kinase Is Inhibited by Covalent Binding.* ACS Chem Biol, 2019. **14**(3): p. 342-347.
25. Guo, W.H., et al., *Enhancing intracellular accumulation and target engagement of PROTACs with reversible covalent chemistry.* Nat Commun, 2020. **11**(1): p. 4268.
26. Zeng M, X.Y., Safaee N, Nowak RP, Donovan KA, Yuan CJ, Nabet B, Gero TW, Feru F, Li L, Gondi A, Ombelets LJ, Quan C, Janne PA, Kostic M, Scott DA, Westover KD, Fischer ES, Gray NS, *Exploring targeted degradation strategy for oncogenic KRAS (G12C).* Cell Chem Biol, 2020. **27**: p. 19-31.
27. Tong, B., et al., *A Nimbolide-Based Kinase Degrader Preferentially Degrades Oncogenic BCR-ABL.* ACS Chem Biol, 2020. **15**(7): p. 1788-1794.
28. Tong, B., et al., *Bardoxolone conjugation enables targeted protein degradation of BRD4.* Sci Rep, 2020. **10**(1): p. 15543.